PCA Energy Response

Abstract

A postscript version is available.

1 Energy Scale

The energy scale can be continuously monitored from the Am^{241} calibration spectra; an example is shown in the lower trace in fig 1. The lines and their intrincsic energies are identified in table 1. Unfortunately, there is no low energy line measured by the continuously available calibration spectrum. A line at 4.1 keV (the Xenon L-escape line) is available from the EDS mode B_32S_256M_0_255_F. This modes was invented for integration and test purposes, and produces ten pulse height spectra for each detector, each with 256 channels. Of particular interest, the column (64 255)—(320 511)—(1088 1279)—(1344 1535)SpecPcu0 contains all events which had the alpha calibration flag set for PCU 0. Most of these events also had a single LLD flag, and are included in the calibration spectra in the Standard 1 data (which requires that only a single LLD flag be set). Some of the events, however, contain 2 LLD flags. A large fraction of these events are due to the detection of an Am^{241} photon and an escape photon. Of these, a few are L-escape photons, and of these events, a fraction of the pulse heights correspond to the L-escape photon. It is not useful to try to estimate these fractions too carefully, but merely to note that in an integration of a few hours, a significant peak at 4.1 keV can be measured. The points of fig 1 shows this spectrum. There is no direct information about which signal chain originated the Xe L escape photons; this peak is assumed to have equal contributions from all layers. (In early December 1996 we are working on a calibration mode to partly resolve this degeneracy.)

Fits to the two spectra give channel numbers which correspond to the lines. The fits are summarized in several tables which cover the 5 detectors and 3 high voltage settings used during the first year of the RXTE mission.

Performing fits to the energy/channel pairs overlooks important and well known physics of gas filled proportional counters as no account is made of discontinuities at the atomic absorption edges. After photoelectric absorption of an x-ray just above an edge, the resulting Xenon ion has, on average, a higher ionization state than when an x-ray just below the edge is absorbed.

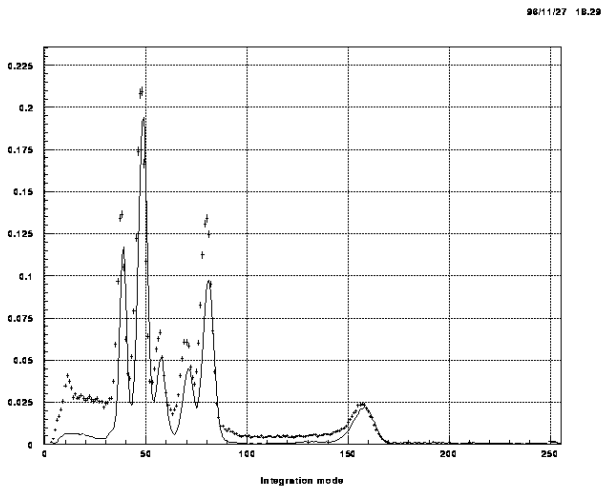

Figure 1: Calibration spectrum from PCU 0. The points are from the Integration and Test mode; the line is the simultaneously obtained Standard 1 data.

Table 1: Calibration line energies

Line number	Energy (keV)	$\frac{E_\gamma}{w(E)}$	Line source
1	4.110	186.47	Xenon L-escape
2	13.925	637.51	Np L_α
3	17.534	804.40	Np L_{beta}
4	21.125	970.85	Np L_{gamma}
5	~ 26		blend Kβ escape from 7 and Am^{241}
6	29.870	1372.75	Kα escape line from 7
7	59.537	2735.71	Am^{241}

Table 2: Fits to epoch 3 calibration lines

Energy	4.110	13.925	17.534	21.125	29.87	59.537
Energy-p	4.102	14.025	17.697	21.359	30.20	60.186
PCU 0 - all	10.98	37.62	47.29	56.46	79.84	156.0
PCU 0 - LR1		37.90	47.70	56.81	80.35	156.6
PCU 0 - LR2		37.60	47.24	56.45	79.68	156.1
PCU 0 - LR3		37.54	47.12	56.26	79.48	155.2
PCU 1 - all	11.53	39.28	49.32	58.80	83.03	162.5
PCU 1 - LR1		38.93	49.02	58.40	82.61	161.4
PCU 1 - LR2		38.86	48.88	58.32	82.49	161.6
PCU 1 - LR3		39.60	49.75	59.44	83.98	164.4
PCU 2 - all	10.81	37.81	47.61	56.87	80.46	157.4
PCU 2 - LR1		37.96	47.81	57.01	80.62	157.5
PCU 2 - LR2		38.51	48.41	57.77	81.52	159.5
PCU 2 - LR3		37.43	47.00	56.12	79.35	155.5
PCU 3 - all	11.80	40.65	51.01	60.81	85.80	167.4
PCU 3 - LR1		40.63	51.05	60.85	85.78	167.0
PCU 3 - LR2		40.64	50.98	60.78	85.81	167.7
PCU 3 - LR3		40.66	51.01	60.80	85.82	167.6
PCU 4 - all	10.60	36.15	45.45	54.17	76.54	149.5
PCU 4 - LR1		36.21	45.58	54.23	76.70	149.8
PCU 4 - LR2		36.26	45.60	54.34	76.78	150.1
PCU 4 - LR3		36.08	45.28	54.02	76.19	148.8

In other words, above the edge, more photon energy goes into potential energy of the ion and less into production of electrons which can participate in the avalanche. Several groups have measured the discontinuites at the Xenon L and K edges ([Santos et al. (1994)], [Santos et al. (1991)], [Bavdaz et al. (1995)], [Tsunemi et al. (1993)]). One approach is to perform a fit to a smooth polynomial with offsets at the absorption edges [Jahoda and McCammon (1988)]. A better approach which is possible for Xenon counters is to estimate the number of electrons produced by each incident photon A series of papers (many refs) studies the detailed response of Xenon to photo-ionization, and tabulates (among many other properties) the quantity $w(E_\gamma)$, defined as the number of eV required per electron. The data come from detailed Monte Carlo models which are well verified by measurement. Fig 2 shows the variation of $w(E_\gamma)$ with photon energy. It is possible to estimate the apparent discontinuity at in the energy to channel conversion from the sharp steps in fig 2; the predicted discontinuity is $\sim$ 100 eV at the L edge and $\sim$ 200 eV at the K edge, in agreement with the measurements cited above.

[Dias et al. (1996)] have discovered, from Monte Carlo calculations, confirmed by measurement, that $w(E_\gamma)$ is not just a function of absorbed energy, but that there are offsets if escape peaks are involved. From their figure 3, we calculate offsets of 3.90, -2.26, and 3.84 electrons for peaks due to L_α, K_α, and K_β escape peaks, respectively. Table 1 includes a column with the average number of electrons involved in each event, including the offset for peak 6. Peak 5 is not included as the relative weights of the two lines in uncertain. Quadratic fits are performed for channel as a function of N(E). For convenience we do this as a function of $22 \times N(E)$ which gives an x coordinate that is close to, though not exactly equal to, incident energy. (This is a convenience for creating a matrix that can be plotted in energy space inside XSPEC).

`Pcarmf` provides the possibility of approximating the energy to channel conversion as either a second order polynomial in energy vs channel or E' vs channel where $\frac{E'=E_\gamma \times 22.0eV}{w(E_\gamma)}$.

2 PCARMF

Here I step through the calculation of the response matrix, with particular attention to parameters which can be changed on the `pcarmf` command line.

Matrix energies

`PCARMF` begins, after reading in parameter values in subroutine `rmffpar`, by setting up the matrix energies. The matrix is evaluated at 900 energies by subroutine `mat_energ`. 450 channels are nearly evenly spaced between 0.023 and 10.0 keV; these channels share boundaries with 447 evenly spaced channels and include three extra boundaries at the Xenon L-edges. The exact energies of the L-edges are input parameters `xeL3edge, xeL2edge, and xeL1edge` with default values of 4.782, 5.104, and 5.453 keV

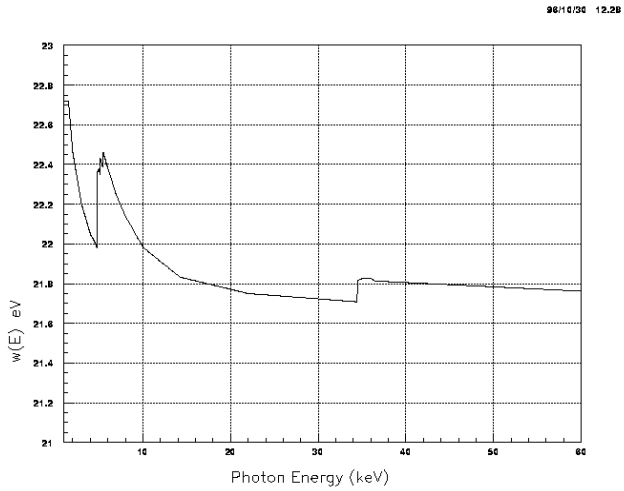

Figure 2: Energy required to create, on average, one thermal electron as a function of incident photon energy.

[X-ray Data Booklet].

450 more energy channels share boundaries with with 449 equally spaced channels between 10.0 and 70.0 keV with an additional channel boundary at the Xenon K-edge which is input as `xeKedge` with default value 34.561 keV [X-ray Data Booklet].

The upper and lower boundaries at which the matrix is evaluated are (version 2.0a) hardcoded, as is the number of allowed edges. Future improvements will create a loagarithmic energy spacing, an arbitrary number of fixed boundaries, and user choosen minimum and maximum energies.

Channel Energies

The matrix is evaluated for 256 channels, which is the full resolution of the PCA Analog to Digital conversion. [1]. The channels are numbered from 0 to 255 (i.e. just the way they emerge from the Analog to Digital converter aboard the instrument.) Neither the on-board Experiment Data System, or the ground data processing tools (XFF, SA(E)EXTRCT) change the channel numbering scheme. `Pcarmf` internally creates a matrix declared as `resp_matrix(0:maxchan-1, maxen)`. Care is taken to ensure that the matrix writing tools and downstream matrix manipulation tools recognize the convention that the first channel element is array element 0.

Although there is no unique mapping of channel to energy due to the fi-

[1] Many users will not obtain 256 channel pulse height spectra, due to gain shifting and rebinning which occurs either on-board or on the ground. Other tools, bundled together in the `pcarsp` script, provide the gain shifting and rebinning as necessary. I regard this as a digital operation associated with channel counting while `pcarmf` addresses the analog operation of creating the full resolution matrix

nite energy resolution of the proportional counters, each channel is given energy boundaries to allow, primarily, plotting of counts vs energy in downstream spectral analysis (typically XSPEC [Arnaud (1996)]). The subroutine `chan_energ` sets the channel bounds by iterative calls to `chan2energy`. The calling sequence indicates whether the upper or lower boundary of a particular channel is requested, so `chan2energy(channel,edge)` returns the energy that corresponds to channel ± 0.5. For `e2c_model=2` (the default) energy is reutrned; for `e2c_model=3` E' is returned.

Efficiency

For each matrix energy, an efficiency is calculated. The efficiency is based on the photoelectric crossections of aluminum, mylar, propane, xenon, and methane. All of the subroutines that return cross sections are based on my own fits to cross section data from [Henke et al. 1982] (energies less than 10 keV) and [Veigele 1973] (energies above 10 keV). All components except xenon are assumed to be transparent above 10 keV. More recent photoelectric cross sections for xenon **??** can be used (up to 30 keV) by specifying `LBL_sigma=1.1` (any number greater than 1.) (Future versions will make this an integer flag). The parameter names and default values are reproted in table 3.

The propane, mylar, and aluminum thicknesses are based on nominal densities. The propane layer is 1.3 cm thick and filled to 798 torr at $20°C$. The mylar windows are nominally 0.0009 inch thick; mylar has a nominal density of 1.4 $\mathrm{gm\,cm^{-3}}$. The nominal aluminum coating is 700 angstroms per side; the bulk density of aluminum is 2.7 $\mathrm{gm\,cm^{-3}}$.

The xenon volume is also made up of layers of nominal 1.3 cm thickness although examination of figure 2 in [Zhang et al. 1994] shows that the arrangement of ground plane wires and the window leaves the first layer with a larger effective depth than the second and third layers. The 5 detectors are allowed to have slightly different amounts of xenon as this can make a difference in the values fit to simple continuum models. A near future release will adjust these values subject to the assumption that all detectors should measure the same spectrum for any object (although note that the individual channel to energy conversions can also affect the details here)

Methane is not treated as a free parameter; the amount of methane is scaled to to be 10% of the amount of xenon by pressure. The results are not very sensitive to this value.

For photons above the K edge, the parameter `xe_kedge_veto` provides a self veto parameterization. For a value of 1 (current default), no self veto is included; for a value of 0.9, 10% of the high energy photons are self vetoed.

Response to mono chromatic input

For each energy, the response observed in each of the 256 channels is caluclated in subroutine `respch`. The response includes the main photo peak, Xenon L escape peak (for energies between the L and K edges), and K_α and K_β escape peaks for energies above the K edge. (In principle, L escape

Table 3: Assumed thickness of detector elements

Parameter name	description	$gmcm^{-2}$
pr_gmcm2	propane in front volume	0.00261
my_gmcm2	mylar thcikness of two windows	0.00508
al_gmcm2	aluminum thickness of four window surfaces	7.6e-5
xe_gm_cm2_l1_p0	xenon in first layer	0.00750
xe_gm_cm2_l2_p0	xenon in second layer	0.0060
xe_gm_cm2_l3_p0	xenon in third layer	0.0060
xe_gm_cm2_pr0	xenon in propane layer	1.27e-04
xe_gm_cm2_l1_p1	xenon in first layer	0.00750
xe_gm_cm2_l2_p1	xenon in second layer	0.0060
xe_gm_cm2_l3_p1	xenon in third layer	0.0060
xe_gm_cm2_pr1	xenon in propane layer	1.82e-04
xe_gm_cm2_l1_p2	xenon in first layer	0.00750
xe_gm_cm2_l2_p2	xenon in second layer	0.00600
xe_gm_cm2_l3_p2	xenon in third layer	0.00600
xe_gm_cm2_pr2	xenon in propane layer	1.34e-04
xe_gm_cm2_l1_p3	xenon in first layer	0.00750
xe_gm_cm2_l2_p3	xenon in second layer	0.0060
xe_gm_cm2_l3_p3	xenon in third layer	0.0060
xe_gm_cm2_pr3	xenon in propane layer	1.37e-04
xe_gm_cm2_l1_p4	xenon in first layer	0.00750
xe_gm_cm2_l2_p4	xenon in second layer	0.0060
xe_gm_cm2_l3_p4	xenon in third layer	0.0060
xe_gm_cm2_pr4	xenon in propane layer	1.85e-04

Table 4: Escape fractions and Offsets

xeKedge	Xenon K edge	34.561
xeL3edge	Xenon L3 edge	4.782
xeL2edge	Xenon L2 edge	5.104
xeL1edge	Xenon L1 edge	5.453
EscFracKb	Xenon K_α escape fraction	0.155
EscFracKa	Xenon K_β escape fraction	0.545
EscFracL1	Xenon L escape fraction (top layer)	0.010
EscFracL2	Xenon L escape fraction (two layer)	0.000
EscFracL3	Xenon L escape fraction (third layer)	0.000
EscFracLt	Xenon L escape fraction (whole detector)	0.009
EscEnerKa	Xenon K_{alpha} energy	29.70
EscEnerKb	Xenon K_{beta} energy	33.62
EscEnerLa	Xenon L_{alpha} energy	4.110
DeltaE_L3	non linearity at L3 edge (keV)	0.085
DeltaE_L2	non linearity at L2 edge (keV)	0.032
DeltaE_L1	non linearity at L1 edge (keV)	0.012
DeltaE_K	non linearity at K edge (keV)	0.180
delta_el_L	offset for L escape photons (electrons)	3.9
delta_el_Ka	offset for K_{alpha} escape photons (electrons)	-2.26
delta_el_Kb	offset for K_{beta} escape photons (electrons)	3.84

peaks should be calculated above the K edge as well; these peaks would only be a shoulder on the edge of the relatively broad main peak.) Resolution is calculated approximately by approximating the resolution for PCU 0 as $1.06 + 0.051 \times E(kev) + 2.4 \times 10^{-4} \times E(kev)^2$ (fit to calibration data from May 1996). This expression gives σ in channels. The value is scaled to other detectors and other high voltage epochs by the ratio of slopes for the energy to channel relations. Table 4 shows the mnemonics and default values for the escape fractions. Since the K escape photons travel a long way (usually out of the detector) the probabilitity is nearly energy independent; the L escape photons on the other hand, have a modest range, and are likely to be reabsorbed if they start in an interior layer. The fraction of interest is not the intrinsic flouresence yield, but the yield times the probability that the escape photon escapes the detector. Strict accounting should check for the fraction of events that are self vetoing; this is only done for the K escape photons in the efficiency calculation.

Both the photopeak and escape peaks are modelled as gaussians. A correction is made for the width of each channel for `e2c_model=2` (For `e2c_model=3` the width of the channels is automatically correctsince the energy to channel conversion will put 'extra' events into the channels near the edges). The correction is calculated in subroutine `chanwidth` and smears the measured jumps at edges (i.e. `DeltaE_L3` over several channels using the estimated resolution function.)

Other required and optional inputs

`Pcarmf` will prompt for the name of the output file `outfile`, the PCU identification `pcuid`, the signal chain identifier `lld_code`, and the date `date`. Allowed values of `pcuid` are 0,1,2,3, or 4. The signal chain identifier is made up of the sum of powers of 2. The L1 signal is designated as 1, R1 as 2, L2 as 4, R2 as 8, L3 as 16, and R3 as 32. If the matrix is created for all "good" events then `lld_code=63` should be specified. Not all combinations are supported; currently `pcarmf` correctly handles any individual anode chain (1,2,4,8,16,32), any layer in the detector (3,12,48), or the entire detector (63). The date is assumed to be a 6 character string of the form `date=960714`. At present the date is used only to distinguish among the 3 distinct high voltage epochs [Jahoda et al. (1996)], although the program could later be expanded to incorporate a gradual time dependence if one is discovered.

The default energy to channel model simply uses quadratic fits to the energy/channel pairs reported in, for instance, 2 `e2c_model=2`. The interpretation based on number of electrons `e2c_model=3` is available, although no coefficients are available for some epochs. New coefficients can be entered through creating a FITS file similar to the ones found in the CALDB (the default for `e2c_file`) or by creating an ascii file with a particular format, illustrated below:

```
C  data file for energy to channel
C
C strict format rules apply:
C    lld specifies lld binary code; m# specifies model number.
C                                      =1 ==> ch = par(1) + par(2)*e
C                                      =2 ==> ch = par(1) + par(2)*e + par(3)*e**2
C yymmdd S# lld m# --par(1)--- -par(2)---- all parameters are 1pe11.4 with 1 space in betwe
C

  960414  0   1  3  3.5705E-01  2.7031E+00 -1.8384E-03
  960414  0  63  3  5.5063E-01  2.6578E+00 -1.1055E-03
```

If `nofits=1`, `pcarmf` reads the ascii file specified by `e2c_file` until it finds an entry that has exact matches for `pcuid, lld_mode,` and `e2c_model` and a `date` that is earlier than the observation. (Using this mode of input requires that the epoch 3 entries precede earlier epochs in the file.) The program will also accept a value of `lld_code=63` (whole detector average) if it comes across such before it finds the specific code. This requires that the entry of `lld_code` come after all other entries for a particular combination of date, pcuid, and model.

For the very brave, there is a possibility to make sweeping changes to the efficiencies. If the parameter `scale_hack=1`, then the file `scale_file=filename` is read for pairs of energy/multiplicative scale factors. All efficiencies calculated by `pcarmf` are multiplied by the linearly interpolated value. Use with

caution, although this feature has been changed in version 2.0a so that it at least does what is advertised here.

Writing the matrix

`Pcarmf` is capable of one compression, and can write out matrices in the Standard 2 format (129 channels) if called with `std2_mx=1` (default is 0). Users of `pcarsp` should avoid this as that script will perform this function via a call to `rbnrmf`.

The matrix is compressed via the ftools callibration subroutines `grprmf`, `wtrmf3`, and `wtebd3`, all of which are relatively recent and allow the user to specify that the first channel of the matrix is numbered 0 (i.e. not 1).

References

[Arnaud (1996)] Aranud, K., 1996, Astronomical Data Analysis Software and Systems V, eds. Jacoby, G. and Barnes, J., p. 17, ASP Conf. Series volume 101.

[Bavdaz et al. (1995)] Bavdaz, M., Martin, D., and Peacock, A. 1995, SPIE 2518, ppp.

[Dias et al. (1996)] Dias, T.H.V.T et al., 1996, IEEE-Trans. Nucl. Sci, in press.

[Henke et al. 1982] Henke, B.L., Lee, P., Tanaka, T. J., Shimabukuro, R. L., and Fujikawa, B. K. 1982, Atomic Data and Nuclear Data Tables, 27, 1.

[Henke et al. 1993] Henke, B. L., Gullikson, E. M., and Davis, J. C., 1993, Atomic Data and Nuclear Data Tables, 54, 181; http://www-cxro.lbl.gov:80/optical_constants/

[Jahoda et al. (1996)] Jahoda, K., Swank, J. H., Giles, A. B., Stark, M. J., Strohmayer, T., Zhang, W., and Morgan, E. H., 1996, SPIE 2808, 59.

[Jahoda and McCammon (1988)] Jahoda, K. and McCammon, D. 1988, Nucl. Instr. and Meth., A272, 800.

[X-ray Data Booklet] Kirz, J. et al., "X-ray Data Booklet", Center for X-ray Optics, Lawrence Berkeley Laboratory, 1986.

[Santos et al. (1991)] Santos, F.P., Dias, T.H.V.T., Stauffer, A.D., and Conde, C.A.N. 1991, Nuclear Instruments and Methods, A307, 347.

[Santos et al. (1994)] Santos, J.M.F., Morgando, R.E., Tavora, L.M.N., and Conde, C.A.N., 1994, Nuclear Instruments and Methods, A350, 216.

[Tsunemi et al. (1993)] Tsunemi, H., Hayashida, K., Torri, K., Tamura, K., Miyata, E., Murakami, H., and Ueno, S., 1993, Nuclear Instruments and Methods, A336, 301.

[Veigele 1973] VEigele, W. J. 1973, Atomic Data Tables, 5, 51.

[Zhang et al. 1994] Zhang, W., Giles, A. B., Jahoda, K., Soong, Y., Swank, J. H., and Morgan, E. H. 1994, SPIE 2006, 324.